

# Aluminum doping of CdTe polycrystalline films starting from the heterostructure CdTe/Al

M. Becerril<sup>a,\*</sup>, O. Vigil-Galán<sup>b</sup>, G. Contreras-Puente<sup>b</sup>, and O. Zelaya-Angel<sup>a</sup>

<sup>a</sup>*Departamento de Física, Centro de Investigación y de Estudios Avanzados del Instituto Politécnico Nacional, Apartado Postal 14-740, México D.F., 07000 México.*

<sup>b</sup>*Escuela Superior de Física y Matemáticas, Instituto Politécnico Nacional, México D.F., 07738 México,*

*\*e-mail: becerril@fis.cinvestav.mx*

Recibido el 18 de mayo de 2009; aceptado el 17 de junio de 2011

Aluminum doped CdTe polycrystalline films were obtained from the heterostructure CdTe/Al/Corning glass. The aluminum was deposited by thermal vacuum evaporation and the CdTe by sputtering of a CdTe target. The aluminum was introduced into the lattice of the CdTe from a thermal anneal to the CdTe/Al/Corning glass heterostructure. The electrical, structural, and optical properties were analyzed as a function of the Al concentrations. It was found that when Al is incorporated, the electrical resistivity drops and the carrier concentration increases. In both cases the changes are several orders of magnitude. From the results, we conclude that, using this deposition technique, *n*-type Al doped CdTe polycrystalline films can be produced.

**Keywords:** Semiconducting II-VI materials; thin films; CdAlTe; radio frequency sputtering.

Películas policristalinas de CdTe dopadas con aluminio fueron obtenidas a partir de la heteroestructura CdTe/Al/Vidrio Corning. El aluminio fue depositado por evaporación térmica en vacío y el CdTe por erosión catódica a partir de un blanco de CdTe. El aluminio fue introducido dentro de la red del CdTe por medio de un tratamiento térmico a partir de la heteroestructura CdTe/Al/Vidrio Corning. Las propiedades ópticas, eléctricas y estructurales fueron analizadas en función de la concentración de aluminio. Se encontró que cuando el Al es incorporado dentro de la red del CdTe, la resistividad disminuye y la concentración de portadores aumenta. En ambos casos los cambios son de varios órdenes de magnitud. De estos resultados se puede concluir que usando estas técnicas de deposición se pueden producir películas policristalinas de CdTe-Al tipo *n*.

**Descriptores:** Materiales semiconductores II-VI; películas delgadas; CdAlTe; erosión catódica.

PACS: 61.10.Nz; 68.37.-a; 73.61.Ga; 78.40.Ha; 81.15.Cd

## 1. Introduction

Doping in semiconductor materials to obtain electron or hole *nor p*-type conductivities is a widely studied phenomenon. The effective doping of a semiconductor material considerably increases its potential applications in the fabrications of technological devices. In the case of polycrystalline semiconductor films, doping is generally more difficult, therefore, it is important the development of new technologies for effective doping. Some intrinsic structural defects in these materials, such as grain boundaries, act as carrier trapping centers, limiting the conductivity of the films. On the other hand, the deposition of polycrystalline semiconductor films using thermal evaporation and sputtering techniques is more economic than the growth of bulk semiconductor materials or than thin layers deposited by techniques such as molecular beam epitaxy (MBE). Thus, an important reduction in the cost of the devices can be achieved by preparing doped polycrystalline thin films with appropriate quality.

Aluminum doping of CdTe polycrystalline thin films deposited on glass substrates has been tried before for many researchers with less success [1]. Aluminum incorporation into CdTe polycrystalline films has been done using several techniques such as physical-vapor transport and vacuum evaporation [2,3] In those cases, the reported values of the resistivity

are either much lower or much higher than at reported in the present letter.

## 2. Sample preparation and experimental details

In this work we have grown aluminum doping of CdTe polycrystalline films starting from the heterostructure CdTe/Al/Corning 7059 glass. The later thermal annealing given to the heterostructure produced a decrease of eight orders of magnitude in the electrical resistivity respect none doping sample and an increase of three orders of magnitude in the carrier concentration when the Al concentration is increased. The layers of aluminum were deposited by thermal vacuum evaporation and the CdTe by sputtering of a CdTe target. The glasses used in the deposition were ultrasonically cleaned, freshly etched with trichloroethylene, acetone, methanol, distilled water, and dried with N<sub>2</sub>. Aluminum films of 5.5, 11.5 and 50 nm thicknesses were coated on Corning glass substrates at room temperature (RT). The deposition pressure was of the order of 10<sup>-3</sup>Torr. The commercial monitor, MASTEK Inc., which uses a crystal resonator as sensor, was used to measure the thicknesses of the aluminum films. Soon after, CdTe polycrystalline films were grown on aluminum thin films at RT in a radio frequency (r.f.) sputtering

TABLE I. Thickness, compositions, electrical, and optical properties of the CdTe-Al films.

Sample	Thickness (Å)	Annealing (350°C)	Al (% at)	Cd (% at)	Te (% at)	$E_g$ (eV)	$E_{Ad}$ (eV)	Mobility ( $\text{cm}^2 \text{V}^{-1} \text{s}^{-1}$ )
CdTe/Al								
B0	1225/ 0.0	–	0.	44.91	55.09	1.50	0.69±0.02	
B1	1237/ 55	t = 40 sec	0.91	46.86	52.23	1.60	0.68±0.02	11.21
B2	1215/ 115	t = 60 sec	1.99	48.93	49.08	1.64		81
B3	1230/ 505	t = 10 min	3.57	47.86	48.57	–		Very low

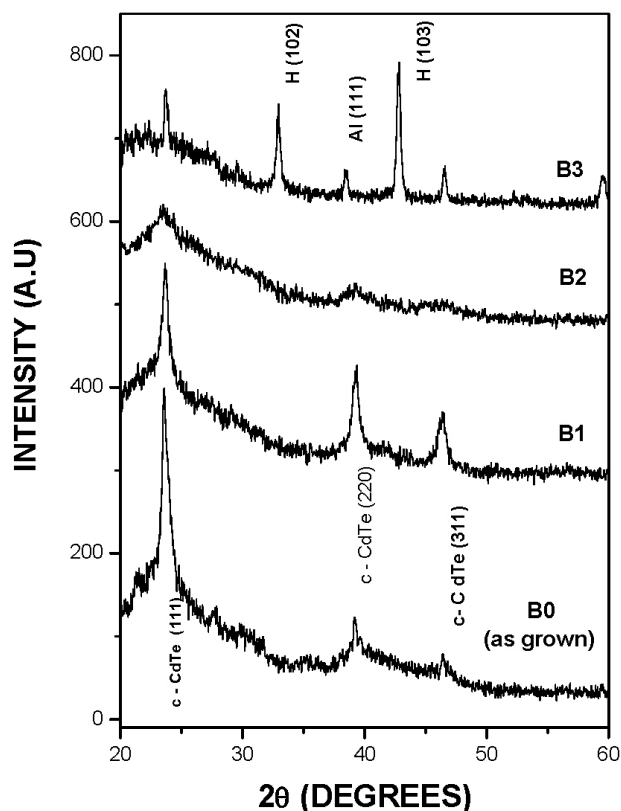


FIGURE 1. X-ray diffractions spectra of B0-B3 samples. The meaning of C and H before the plane indexes is cubic and hexagonal, respectively.

system. The rf power used in the grown process was 40 W and the distance between target and substrate was 4 cm. High purity argon gas was used to obtain the sputtering plasma. The initial pressure in the chamber was  $1 \times 10^{-5}$  Torr, and the final pressure of the argon plasma was about  $10^{-3}$  Torr. A deposition time of 3 h was used for all the growths. The CdTe (99.999% pure) target had an area of  $4.92 \text{ cm}^2$ . The thickness of CdTe films was about 120 nm. The samples CdTe/Al (0.0, 5.5, 11.5 and 50 nm) were denoted by B0, B1, B2 and B3, respectively.

With the purpose that the aluminum diffused in the lattice of the CdTe, a thermal annealing was given to the Bn samples in an argon atmosphere at 350°C (see Table I for details of annealing). Higher values than  $T = 350^\circ\text{C}$  and annealing times

of 10 min affected sensitively the thickness of the films. The thickness of CdTe films were measured by a KLA TENCO P-15 profilometer. Film composition was measured by energy dispersion spectroscopy (EDS) using a Perkin-Elmer (JSM-6300) system. The crystalline structure of the films was determined from X-ray diffraction (XRD) patterns, measured with an X-ray SIEMENS D5000 diffractometer. The electrical properties in dark were measured as a function of temperature using a 4600 BIO-RAD, DLTS spectrometer. For data measurements CdTe/Al films were heated at 0.15 K/s from 100 to 450 K with an applied bias voltage of 10 V. The dark current signal was measured with a programmable 617 KEITHEY electrometer connected to a 465 GOULD oscilloscope. The carrier concentration, mobility and type of conductivity of the films were measured at RT using the Van der Pauw method. In order to perform electrical measurement indium electrodes were deposited on CdTe/Al films. The I-V plots, in the range 0.1-10 volts, obtained with this method were linear, indicating ohmic behavior of the contacts in all samples. The optical absorption spectra of the films were measured by a UNICAM 8700 spectrophotometer.

### 3. Experimental results and discussion

The X-ray (XRD) diffractions spectra of the five samples are shown in Fig. 1. The B0 sample corresponds to the composition of a pure CdTe polycrystalline films. The diffraction peaks characteristics of the cubic structure of CdTe (zincblende) are observed at  $23.6^\circ$ ,  $39.2^\circ$ , and  $46.4^\circ$  correspond to the (111), (220), and (311) crystalline planes of this phase, respectively. After annealing, the diffraction lines in the spectra of the B1 and B2 samples, with higher Al contents, exhibit a gradual broadening and a decrease in their intensity, the later indicates a decrease in the crystalline quality in these films, including a reduction in particle size. The patterns for B3 sample exhibit additional diffraction lines corresponding to the hexagonal structure of CdTe and to the metallic aluminum cubic phases. The appearance of the aluminum phase coincides with the abrupt increasing in the aluminum concentration as shown in Table I. The analysis of the chemical compositions and the X-ray data indicates that in samples from B1 and B2, the Al atoms are incorporated into the Cd sites in the CdTe lattice. In the B3 sample, the aluminum concentration increases abruptly causing segregation of three

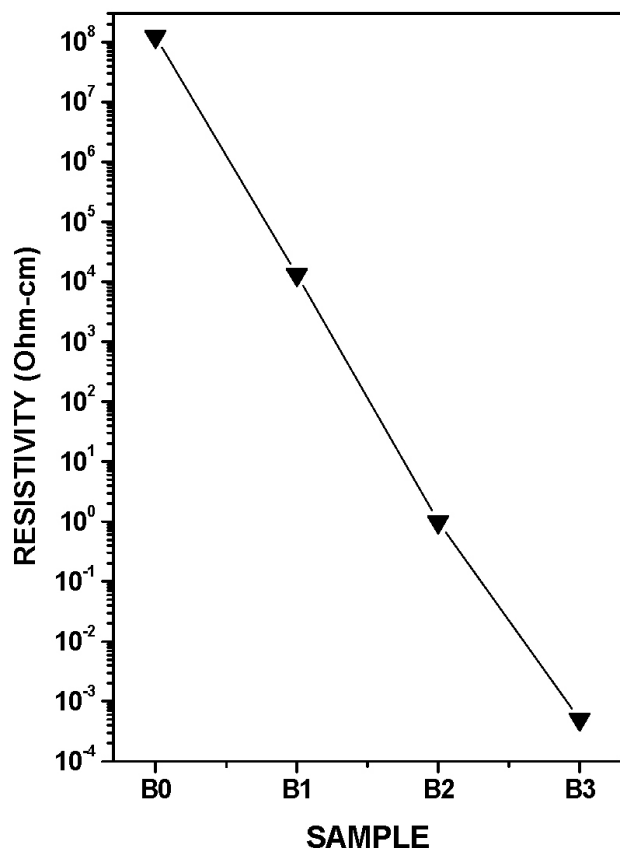


FIGURE 2. Dark electrical resistivity of the B0-B3 samples.

different phases, c-CdTe, h-CdTe and c-Al. The existence of  $\text{Al}_2\text{Te}_3$  was not observed in the films in XRD patterns. Work of other authors on CdTe:Al with up to  $\sim 20$  at% of Al in samples also does not report the presence of  $\text{Al}_2\text{Te}_3$  in films prepared by close spaced transport [4]  $\text{Al}_2\text{Te}_3$  is thermodynamically more stable than CdTe, however, Al atoms are not in contact with free Te during the growth and annealing processes.

The room temperature electrical resistivity ( $\rho$ ) and carrier concentration of the Bn samples are shown in Fig. 2 and Fig. 3, respectively. As can be seen, the incorporation of aluminum into the CdTe films has a strong effect in both electrical parameters. The resistivity of the samples B1 and B2 drops by four and eight orders of magnitude, respectively, as compared to that measured in the pure CdTe (B0) sample. The sudden changes in the resistivity of the sample B3 coincide with the formation of the conductive phase in the films, Al (100). The value of resistivity of B3 film is of the same order as those observed in metallic materials. However, it can be observed that an abrupt change in carrier concentration occurs for the B3 sample, which coincides with the appearance of the metallic phase in the film, Al (100). The above mentioned results indicate that Al is effectively doping the CdTe films and according to the Hall measurements is *n*-type, due to the fact that Al, an element of group III, acts as a donor by substituting Cd atoms. On the other hand, usually, none-doping samples have *p*-type conductivity. With the doping further-

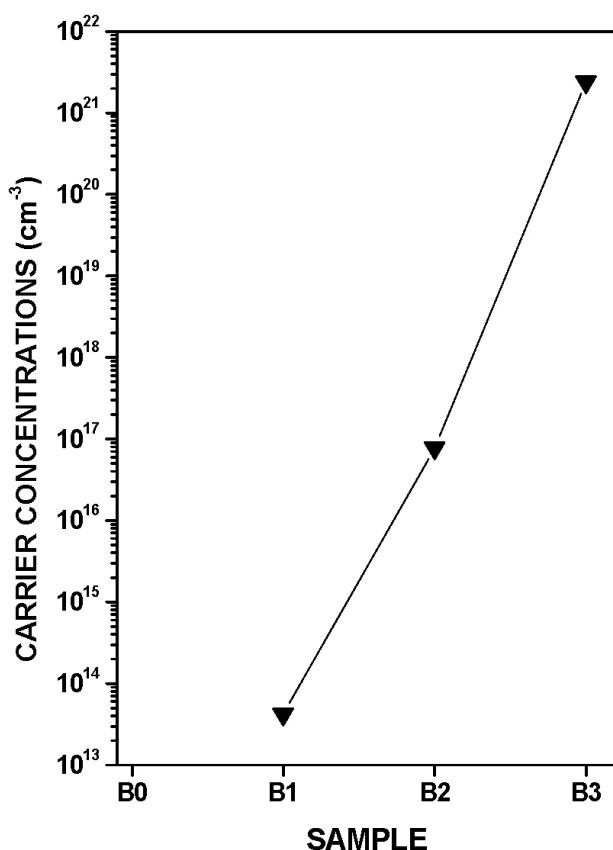


FIGURE 3. Carrier concentration of the B0-B3 samples.

more the change of type of conductivity, a drastic change in the conductivity value is observed, and therefore the aluminum atoms in interstitial sites of CdTe lattice must be taken into account.

Figure 4 shows the behavior of the electrical dark current ( $I_D$ ) as a function of the inverse of absolute temperature ( $T$ ) for the Bn samples. This figure illustrates resistivity versus  $1/K_B T$  data of CdTe films (B0-B2) having a semiconductor behavior, and of a multiphase film (B3) having a metallic behavior. The top inset of Fig. 4 illustrates the dependence of the dark current with  $1/K_B T$  of B3, where the decreasing of  $I_D$  as  $T$  increases is evident. The calculated activation energy, in the RT region, for films B0 and B1 is  $0.69 \pm 0.02$  eV and  $0.68 \pm 0.02$  eV, respectively, which could be ascribed to a native defect level near to the middle of the band gap. For B2, the activation energy does not have constant values, changes with  $T$  in all the range studied. When  $1/K_B T > 26$  eV<sup>-1</sup> ( $T > 450$  K) the B2 sample experiences a Mott transition, *i.e.*, a semiconductor-metal transition due to the high doping concentration, as can be observed in the bottom inset of Fig. 4. The results in this figure support the conclusions about the electrical carrier transport mechanism in the Bn films, particularly the electrical percolation through the aluminum phase in the B3 sample. Notice that for the B1 and B2 samples there is a significant deviation from the straight line behavior in the low temperature range, in this region the conductivity in CdTe can be dominated by shallow donor

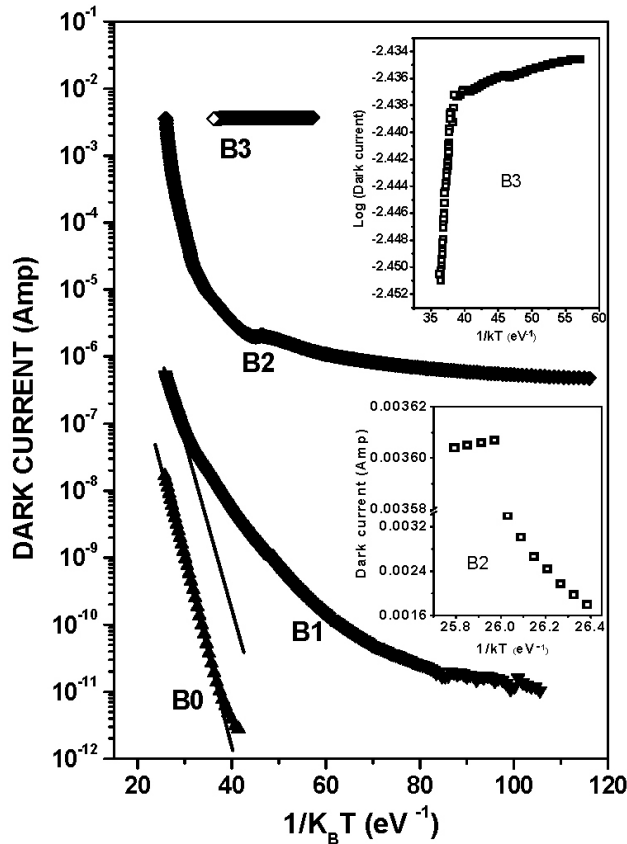
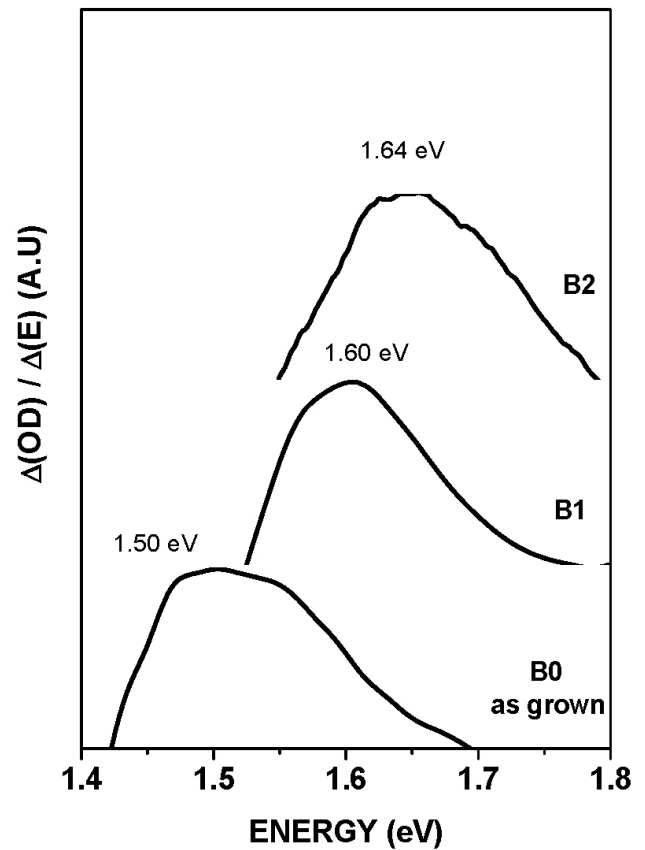
FIGURE 4. Dark electrical current vs.  $1/K_B T$  of Bn samples.

FIGURE 6. Numerical derivative of the absorption spectra of several Bn samples.

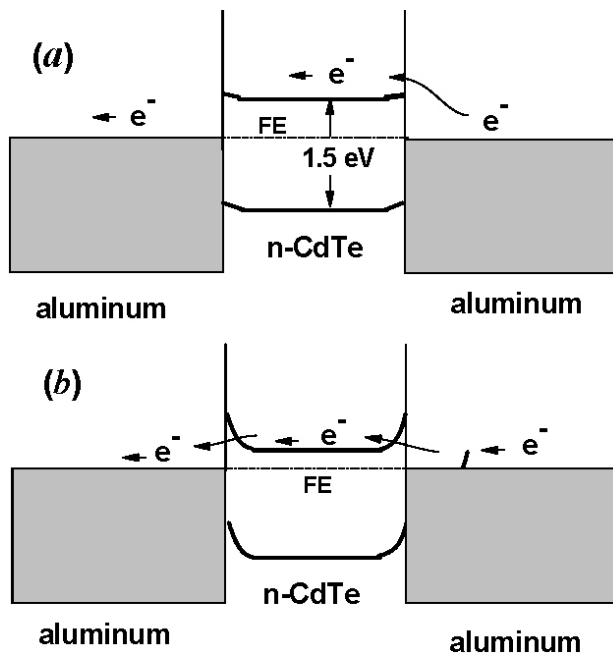


FIGURE 5. Grain boundary of Al/n-CdTe films. (a) Low diffusion Al-atoms density. (b) High Al-atoms diffusion density.

levels In the region  $T \geq 290$  K ( $1/K_B T \leq 40$  eV $^{-1}$ ) the mobility ( $\mu$ ) in B2 has a strong increase as T rises due to the dependence  $\mu \propto T^{3/2}$  of the impurity scattering (see Table I) The behavior of  $I_D$  versus  $1/K_B T$  is similar to that observed for heavily Te doped GaAs (*n*-type) [5]. The bulge around 50 eV $^{-1}$  in B2 has been associated to Cd vacancies in CdTe [6].

The process of transport of carriers between grains through segregated Al at the grain boundaries is illustrated in Fig. 5. CdTe of B1, B2 and B3 films is *n*-type as determined from Hall effects measurements. The barrier height in junctions has been reported equals 0.61 eV [7,8]. Besides, by taking into account the works of Refs. 9 and 1, the Al-CdTe(*n*-type) junction is such as described in Fig. 5(a) for low time diffusion of Al (B1 sample) and in Fig. 5(b) for higher time diffusion of Al. As diffusion time increasing the doping concentration increases in such a way that the Fermi energy (FE) moves toward the conduction band. The junction is rectifier from Al to *n*-CdTe and ohmic in the opposite direction. For very higher doping level, the barrier becomes thinner and tunnelling of electrons increases and, therefore, increasing  $I_D$ .

The numerical derivative of the optical absorption spectra of several samples is plotted in Fig. 6. The peak at about 1.50 eV is due to the electronic transitions from the fundamental energy band edge ( $E_g$ ). The position of the peak has

been used to estimate the  $E_g$  value [11]. In this figure it is observed that the position of the peak shifts toward higher energy values when the aluminum concentration increases in the CdTe films, as is shown in Table I. It is important to mention that c-CdTe and h-CdTe have similar values of  $E_g$  [12]. In this table a shifts in the band-gap value of 100 and 140 meV of the B1 and B2 samples, respect the B0 ones is observed. In other words, for the fundamental optical band gap, a blue shift is observed with respect to the doping concentration which can be explained by the Burstein-Moss effect and therefore the optical properties confirm the electrical one respect an effective aluminum doping process in CdTe from our experimental conditions [13].

#### 4. Conclusions

In conclusion, in this work we have shown that n-type polycrystalline CdTe films, with changes in the electrical resistivity of eight orders of magnitude can be obtained by aluminum

doping, depositing CdTe films by sputtering technique onto Al/Corning glass substrates, where the aluminum is deposited by thermal vacuum evaporation. In this way, to incorporate aluminum in the lattice of the CdTe it was necessary to carry out a post thermal annealing n-type polycrystalline CdTe films doped with Group III elements could be suitable for application in X- and gamma-ray detection if some parameters like resistivity, photosensitivity, response time and carrier lifetime are controlled.

#### Acknowledgments

The authors thank M. Guerrero, H. Silva and J.A. García for their helpful technical assistance. This work was partially support by CONACYT and ICyTDF from México.

- 
1. M. Gonzalez-Alcudia, M. Zapata-Torres, M. Meléndez-Lira, and J.L. Peña, *Rev. Mex. Fís.* **52** (2006) 48.
  2. W. Palosz *et al.*, *J. Electron. Mater.* **32** (2003) 747.
  3. S. Lalitha, R. Sathyamoorthy S. Senthilarasu, A. Subbarayan, and K. Natarajan, *Sol. En. Mater. Sol. Cells* **32** (2004) 187.
  4. M. González-Alcudia, M. Zapata-Torres, M. Meléndez-Lira, and J. L. Peña, *Rev. Mex. Fis.* **52** (2006) 48.
  5. T.K. Saxena, S. Bala, S.K. Agarwal, P.C. Mathur, and K.D. Chauduri, *Phys. Rev. B* **22** (1980) 2962.
  6. M. Becerril, O. Zelaya-Angel, J.R. Vargas-Garcia, R. Ramírez-Bon and J. González-Hernández, *J. of Physics and Chemistry of Solids* **62** (2001) 1081.
  7. I.M. Dharmadasa *et al.*, *Solid-St. Electron* **42** (1998) 595.
  8. P.C. Sarmar and A. Rahman, *Bull. Mater. Soc.* **24** (2001) 411.
  9. L. A. Kosyachenko *et al.*, *J. Appl. Phys.* **101** (2007) 013704.
  10. J.A. Spies *et al.*, *Sol. En. Mater. Sol. Cells* **93** (2009) 1296.
  11. B.G. Potter Jr, J.H. Simmons, *Phys. Rev. B* **37** (1988) 10838.
  12. S.K. Pandey *et al.*, *Thin Solid Films* **473** (2005) 54.
  13. M.Z.I Gering and K.B. White, *J. Phys. C: Solid State Phys.* **20** (1987) 1137.